

# Multiple-beam Ramsey interference and quantum decoherence

M. Mei<sup>1</sup>, M. Weitz<sup>1,2</sup>

<sup>1</sup>Max-Planck-Institut für Quantenoptik, Hans-Kopfermann-Str. 1, 85748 Garching, Germany

<sup>2</sup>Sektion Physik der Universität München, Schellingstr. 4, 80799 München, Germany

Received: 27 July 2000/Published online: 6 December 2000 – © Springer-Verlag 2000

**Abstract.** We study the effect of photon scattering from a path of a four-beam atomic interference setup, which is based on a cesium atomic beam and two subsequent optical Ramsey pulses projecting the atoms onto a multilevel dark state. While in two-beam interference, any attempt to keep track of an interfering path reduces the fringe contrast, we demonstrate that photon scattering in a multiple-path arrangement cannot only lead to a decrease, but – under certain conditions – also to an increase of the interference contrast. The results are confirmed by a density-matrix calculation. We are aware that in all cases the “which-path” information carried away by the scattered photons leads to a loss of information that is contained in the atomic quantum state. An approach to quantify this “which-path” information using observed fringe signals is presented; it allows for an appropriate measure of quantum decoherence in multiple-path interference.

**PACS:** 03.65.-w; 03.75.Dg; 32.80.-t

One of the most striking features of quantum mechanics is that a microscopic particle can exist in a superposition of two (or more) different eigenstates, as, for example, two different spatial locations. Any attempt to measure the particle eigenstate causes a back-action onto the particle, as expressed in several gedanken experiments on wave-particle duality dating back to the early days of quantum mechanics [1]. For example, in a variant suggested by Feynman [2], an electron wavepacket passes simultaneously through two slits and forms an interference pattern which manifests the wave nature. However, if one is trying to obtain “which-path” information, as, e.g., by scattering a photon off the electron, the interference pattern is destroyed. This behaviour is suggested by complementarity. The photon scattering causes a coupling to the environment with its large number of degrees of freedom. The incomplete knowledge about the environment (and, indeed, all macroscopic systems) requires an averaging over the degrees of freedom, causing quantum superpositions to decohere into classical probability distributions. In

recent experimental works, atoms have proven to be attractive candidates for experimental investigations of the wave-particle duality and quantum decoherence [3–6]. As decoherence effects are believed to be responsible for the transition between (microscopic) quantum systems and classical systems, their study in quantum systems of increasing size is of interest [7–9].

In this paper, we report on an interference experiment based on four internal states of the cesium atom in a four-path Ramsey setup. While in a two-beam interference experiment the observation of a path always reduces the fringe contrast [10], this is not necessarily the case in a multiple-beam arrangement. We demonstrate that the scattering of a photon off one of the four paths can also lead to an increase in the Michelson fringe contrast. This non-intuitive situation can occur when one attempts to observe a path in an interferometer where the phase difference between adjacent paths is not constant for all paths. In all cases, the scattering of photons leads to a loss of information contained in the atomic quantum state, as “which-path” information is carried away by the photon field. This missing information over the atomic quantum state – corresponding to a nonzero entropy – shows up as decoherence for the atomic degrees of freedom. Our results suggest that in multiple-beam interference a single Michelson fringe contrast is not sufficient to quantify decoherence. As a measure of the “which-path” information carried away by the photon field, we show that the possible path guessing likelihood [10, 11] always increases with a scattering of photons for the multiple-beam arrangement.

Our experiment employs a multiple-path generalization of a Ramsey experiment in a cesium atomic beam apparatus using optical beams as atomic beamsplitters. Four paths in state space are realized using different magnetic sublevels ( $m_F = -3, -1, 1, 3$ ) of the  $F = 3$  hyperfine component of the cesium electronic ground state, as shown in Fig. 1. During a first optical pulse, cesium atoms are pumped into a dark coherent superposition of the sublevels. This coherent superposition can be probed with a second optical pulse, which again projects the atoms onto a dark state. We observe a sharp Airy-function-like interference signal in the number of atoms

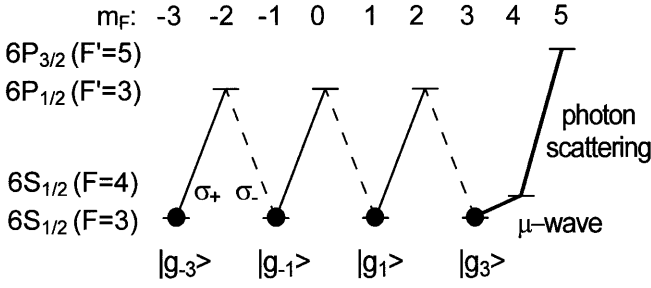


Fig. 1. Schematic of relevant energy levels of the cesium atom

remaining dark in the second pulse as a function of the phase of the second Ramsey pulse [12]. Between the Ramsey interactions, the  $m_F = 3$  path can be observed by applying a suitable combination of microwave transfer pulses and an optical pulse to scatter photons on a closed cycling transition.

The aim of this paper is to give a more detailed account of our previous work on controlled decoherence [13]. In Sect. 1, we outline a theoretical description of the expected fringe pattern using a density matrix approach. In Sect. 2, the experimental setup is described. Experimental fringe patterns for the multiple-beam Ramsey experiment are shown in Sect. 3. In Sect. 4, we present spectra recorded where photons were scattered off an interfering path. The fringe patterns are analyzed and the results are compared to the well-known case of two interfering paths.

## 1 Theory

In the following, we consider an atom with a transition from a ground state of total angular momentum  $F$  to an excited state with total angular momentum  $F'$ , which is irradiated with two copropagating laser beams of  $\sigma^+$  and  $\sigma^-$  circular polarization and frequencies  $\omega_+$  and  $\omega_-$  respectively. We assume that  $F' = F$ , since then a single non-absorbing dark state exists. This dark state has  $N = F + 1$  components with only even (or only odd) magnetic quantum numbers, and a multiple-beam Ramsey experiment with  $N$  paths can be realized using such a transition. We use an interaction picture where the atomic eigenenergies are factored out of the Hamiltonian, such that there is no time evolution of the atomic quantum state between the optical pulses. In the first Ramsey pulse, performed at  $t = 0$ , the atoms are optically pumped into the non-absorbing dark coherent superposition,

$$|\psi_D(0)\rangle = |\psi_{\text{atom}}\rangle = \sum_{n=1}^N c_n |g_{2n-(N+1)}\rangle, \quad (1)$$

with  $|g_{2n-(N+1)}\rangle$  describing a ground state of magnetic quantum number  $m_F = 2n - (N + 1)$ . Note that for  $\omega_+ \simeq \omega_-$  and copropagating laser beams there is no noticeable spatial splitting between the paths. The weights  $c_n$  should be such that  $|\psi_D\rangle$  does not couple to the light field, which yields

$$c_n = c_1 \left( \frac{-\Omega_+}{\Omega_-} \right)^n \cdot \frac{C_{-N+1}^{-N+2} C_{-N+3}^{-N+4} \cdots C_{2n-(N+3)}^{-2n-(N+2)}}{C_{-N+3}^{-N+2} C_{-N+5}^{-N+4} \cdots C_{2n-(N+1)}^{-2n-(N+2)}}, \quad (2)$$

where

$$\begin{aligned} \Omega_+ C_{m_F}^{m_F+1} &= \frac{e}{\hbar} \langle e_{m_F+1} | \mathbf{r} \cdot \mathbf{E}_{0,+} | g_{m_F} \rangle, \\ \Omega_- C_{m_F}^{m_F-1} &= \frac{e}{\hbar} \langle e_{m_F-1} | \mathbf{r} \cdot \mathbf{E}_{0,-} | g_{m_F} \rangle, \end{aligned} \quad (3)$$

with  $C_{m_F}^{m_F'}$  as the Clebsch–Gordan coefficients of the transition from the ground state  $|g_{m_F}\rangle$  to the excited state  $|e_{m_F'}\rangle$ . The factors  $\Omega_+$  and  $\Omega_-$  denote the Rabi frequencies of the  $\sigma^+$  and  $\sigma^-$  polarized waves respectively for a transition with a Clebsch–Gordan coefficient of unity ( $\mathbf{E}_{0,+}$  and  $\mathbf{E}_{0,-}$  stand for the amplitude of the light field). For these weights  $c_n$  the absorption amplitudes into the upper electronic states cancel. The weight  $c_1$  can be chosen to normalize  $|\psi_D\rangle$ . In the following, we assume that  $\Omega_+ = \Omega_-$  at all times, which will result in a symmetric dark state.

Let us initially assume that no attempt is made to detect a path within the interferometer. In this case, a wavefunction approach is sufficient. The first pumping pulse ends at time  $t = 0$  and leaves the atom in the coherent superposition given by (1). The coherent superposition is probed after a time  $T$  with a second Ramsey pulse again projecting the atoms onto the dark state. This pulse is applied with a phase of one of its beams (e.g. the  $\sigma^+$ -polarized component) shifted by  $\phi$ , and the dark state at this time is

$$|\psi_D(T)\rangle = \sum_{n=1}^N c_n e^{-i\varphi(T)(n-1)} |g_{2n-(N+1)}\rangle, \quad (4)$$

where  $\varphi(T) = (\omega_+ - \omega_- - \omega_A)T + \phi$  and  $\omega_A$  denotes the Zeeman splitting between two adjacent even (or odd)  $m_F$  levels. The second pulse will remove most of the population that is not in the dark state. After a few fluorescent cycles these atoms will be pumped to another hyperfine ground state, which is not detected any more. The part that remains in a superposition dark for the light field is the projection

$$\langle \psi_D(T) | \psi_{\text{atom}} \rangle = \sum_{n=1}^N c_n^2 e^{i(n-1)\varphi(T)}, \quad (5)$$

where we have neglected a small fraction that is repumped into the dark state. The interference signal is given by  $|\langle \psi_D(T) | \psi_{\text{atom}} \rangle|^2$ . With no additional phase ( $\phi = 0$ ) and if the driving laser fields are exactly tuned to the two-photon resonance, the atom is still in the dark state at this time. When, for example, the phase of the second pulse is varied, the atom will, in general, be in a coherent superposition of the dark state and the coupled states. The atom is only completely dark after the second pulse if the relative phase between the light field and the atoms has precessed by an integer multiple of  $2\pi$ . One expects an Airy-function-like interference signal with sharp principal maxima in the number of atoms remaining in the dark state [12].

When light is scattered on the  $N$ th path, a detection of the scattered photons would allow one to obtain knowledge about this path. The path can therefore only contribute incoherently to the interference pattern and we expect that the fringe signal reduces to that of a  $(N - 1)$ -way interference pattern. Further, the incoherent background from the  $N$ th path leads to a reduction of the fringe contrast. A calculation of such a signal with partial coherence requires the use of the density matrix.

Let us rewrite the particle wave function before the pulse (1) as

$$|\psi_{\text{atom}}\rangle \equiv |\psi_{\text{part}}\rangle + c_N |g_N\rangle, \quad (6)$$

where  $|\psi_{\text{part}}\rangle = \sum_{n=1}^{N-1} c_n |g_{2n-(N+1)}\rangle$  (note that in general  $\|\psi_{\text{part}}\|^2 < 1$ ). The photon scattering can be described as the coupling of the atom to a detector state [14], after which the total wavefunction is

$$|\psi\rangle \equiv |\psi_{\text{part}}\rangle |D_2\rangle + c_N |g_N\rangle |D_1\rangle, \quad (7)$$

where the state  $|D_2\rangle = |0\rangle$  corresponds to no scattered photons and  $|D_1\rangle = a |D_2\rangle + \sqrt{1-a^2} |D_2o\rangle$ . Here,  $|D_2o\rangle$  is a superposition of continuum states corresponding to one or more scattered photons with  $\langle D_2 | D_2o \rangle = 0$ . The overlap of the two detector states  $\langle D_2 | D_1 \rangle = a$  quantifies the coupling to the environment. For  $a = 1$ , no photons are scattered and full coherence is maintained, while the case of  $a = 0$  corresponds to a complete coupling of the  $N$ -th path to the continuum of photon modes, i.e. the full possible “which-path” information on this path.

We can evaluate the density matrix of the atomic quantum state by tracing over the photon degrees of freedom, which yields

$$\begin{aligned} \rho_{\text{atom}} &= \text{Tr}_{\text{light}}(|\psi\rangle\langle\psi|) \\ &= |\psi_{\text{part}}\rangle\langle\psi_{\text{part}}| + a (c_N |g_N\rangle\langle\psi_{\text{part}}| \\ &\quad + c_N^* |\psi_{\text{part}}\rangle\langle g_N|) + |c_N|^2 |g_N\rangle\langle g_N|. \end{aligned} \quad (8)$$

Thus, by omitting the “which-path” information contained in the scattered photons, the quantum state is converted into a mixed state. The signal with  $a = 0$  describes the case of a complete vanishing of all density matrix diagonal elements related to the  $N$ th path. The interference signal

$$I(\varphi) = \langle \psi_D(T) | \rho_{\text{atom}} | \psi_D(T) \rangle, \quad (9)$$

can be written as

$$I(\varphi) = I_{\text{part}}(\varphi) + a I_{N \leftrightarrow \{1,2,\dots,N-1\}}(\varphi) + |c_N|^4, \quad (10)$$

where  $I_{\text{part}}(\varphi)$  corresponds to the interference of the  $N-1$  paths (e.g. for  $N = 4$  this corresponds to  $m_F = -3, m_F = -1$

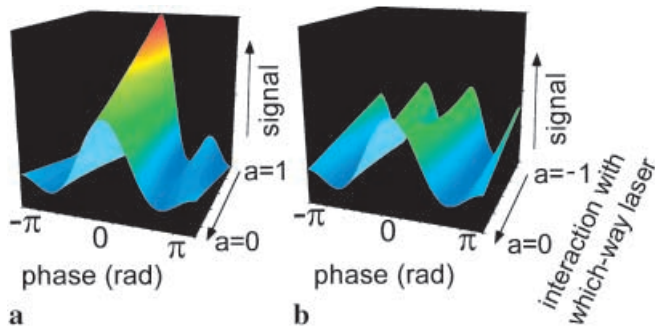


**Fig. 2a,b.** Theoretical fringe pattern for a four-way interferometer **a** with constant phase differences between adjacent paths and **b** with an additional phase shift of  $\pi$  in one outer path. For correspondence with our experiment, the fringe patterns are derived assuming that the interfering probability amplitudes for the two outer paths are a factor 5/3 above those of the two inner ones

and  $m_F = 1$ ),  $I_{N \leftrightarrow \{1,2,\dots,N-1\}}(\varphi)$  to the signal arising from the interference of path  $N$  (for  $N = 4$  this would be  $m_F = 3$ ) with paths  $1, 2, \dots, N-1$  and  $|c_N|^4$  to a background arising from path  $N$  alone. Figure 2a shows a calculated fringe signal for  $N = 4$  paths and different couplings to the environment. For perfect isolation from the environment (i.e. no photons are scattered on the 4th path)  $a = 1$ , and one obtains a four-way interference signal with high contrast and small fringe width. As the coupling to the environment is increased, the contrast decreases and the width of the principal maxima broadens. For full coupling ( $a = 0$ ) to the environment, one obtains a three-way interference signal with an additional incoherent background from the 4th path.

Let us now consider the case of an experiment performed with the phase of the 4th path shifted by  $\pi$ . In this case, all interference terms with the path 4 change sign. We can account for this phase change by choosing a negative prefactor  $a$  to  $I_{4 \leftrightarrow \{1,2,3\}}(\varphi)$  in (10). When no photons are scattered  $a = -1$ , which corresponds to the signal shown in the very back of the 3D plot in Fig. 2b with small amplitude and a minimum at zero phase, corresponding to an inverted contrast. If we scatter photons on path 4, this path will contribute more and more incoherently to the signal, and for full coupling to the environment, one obtains the same signal as in Fig. 2a with  $a = 0$ . This corresponds to the counterintuitive situation of a larger fringe contrast with increased photon scattering, shown in Fig. 2b for different couplings to the environment.

## 2 Experimental setup

Our experimental setup is shown schematically in Fig. 3. In a vacuum chamber, cesium atoms are emitted from an oven and form a thermal atomic beam. The atoms enter a magnetically shielded region, in which they can interact with a series of optical and microwave pulses. A homogeneous 0.54 G magnetic bias field is applied oriented along the optical beams. To induce transitions between atomic sublevels, the atoms are irradiated by optical pulses consisting of two copropagating beams in a  $\sigma^+ - \sigma^-$  polarization configuration tuned to the  $F = 3 \rightarrow F' = 3$  component of the cesium D1 line. Typically, these pulses are 15  $\mu\text{s}$  long. During a first Ramsey pulse, the atoms are optically pumped into a nonabsorbing “dark” coherent superposition of the four ground state Zeeman sublevels with magnetic quantum numbers  $m_F = -3, -1, 1$  and 3 of the  $6S_{1/2}(F = 3)$  ground state. This coherent superposition is probed with a second projection pulse after a time  $T$ , at which interference is observed [12, 15]. The phase of the second Ramsey pulse can be varied during the pulse sequence. The number of atoms left in the dark state after the second optical pump-

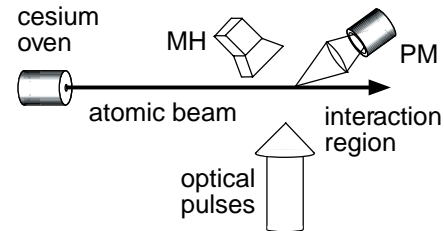


**Fig. 3.** Experimental setup. PM: photomultiplier tube, MH: microwave horn

ing pulse is measured by irradiating the atoms with an optical detection beam tuned to the  $6S_{1/2}(F=3) - 6P_{3/2}(F'=2)$  transition and collecting the fluorescence on a photomultiplier tube. As this transition is not a cycling transition, we maximize the number of scattered photons by varying the polarization of the detection beam with a Pockels cell driven by a radiofrequency of a few MHz. This beam copropagates with the thermal atomic beam to allow Doppler selection of slowly moving atoms.

Between the Ramsey interactions, a coupling to the environment can be achieved for the  $m_F = 3$  path using the following pulse sequence: a microwave  $\pi$  pulse resonant with the  $6S_{1/2}(F=3, m_F=3) - 6S_{1/2}(F=4, m_F=4)$  transition first transfers this component into the other hyperfine sub-level. The microwave pulses are derived from a microwave antenna connected to a radio-frequency (RF) synthesizer. For our magnetic bias field, the microwave transfer was observed at a frequency of 9193.830 MHz. We then irradiate the atoms with a  $\sigma^+$ -polarized optical pulse of variable length resonant with the closed cycling  $F=4 \rightarrow F'=5$  component of the cesium D2 line in order to scatter photons. Subsequently, the atoms are irradiated with a second microwave  $\pi$ -pulse inducing transfer between the hyperfine components and bringing the path back into the ground state level  $F=3, m_F=3$ . Thus, by the time of the second Ramsey interaction, the atoms are in the same internal level as they were before the microwave pulses.

The double microwave transfer induces a phase shift of  $\pi$  for the  $m_F = 3$  path. For some of the experimental spectra, we have compensated for this effect by introducing an additional  $\pi$  phase shift for the second microwave pulse, resulting in an overall phase shift of  $2\pi$  with no observable effect. In addition to this pulse sequence for photon scattering, we irradiated the atoms with a  $\sigma^-$ -polarized repumping pulse tuned to the  $6S_{1/2}(F=4) - 6P_{3/2}(F'=4)$  transition of the cesium D2 line during and a few microseconds after the first Ramsey pulse. This light removes all the population of the intermediate state  $F=4, m_F=4$  before the microwave pulse sequence.

### 3 Multiple-beam Ramsey spectroscopy

Before moving to our studies of quantum decoherence, let us discuss the technique of multiple-beam Ramsey interference [12]. For these measurements, an initial Ramsey pulse generates a coherent superposition of four Zeeman sublevels, which is then probed by a subsequent Ramsey pulse, all other optical and microwave pulses being omitted. A typical recorded spectrum is given in Fig. 4, which shows the number of atoms in the dark state after the second Ramsey pulse as a function of the phase of this pulse. One observes a sharply peaked four-way interference signal with two side maxima. The spectrum was recorded using a time  $T = 68 \mu\text{s}$  between successive light pulses. In order to allow a measurement of the number of atoms in the dark state that is free from background due to, for example, stray optical light, we have determined the background level experimentally by recording the signal measured with an additional two-photon detuning of typically 300 kHz for the Raman beams in the first Ramsey pulse before and after each spectrum. After subtraction of the measured background, the fringe contrast of the experimen-

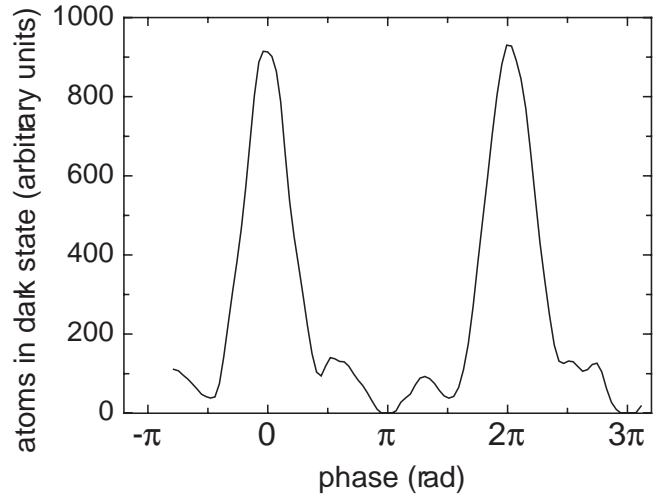


**Fig. 4.** Multiple-beam interference spectrum recorded with a sequence of two Ramsey pulses projecting the atoms onto a multilevel dark state. The plot gives the number of atoms in the dark state after the pulses as a function of the phase of the second Ramsey pulse

tal signal is very close to unity (Fig. 4). The observed width of the principal maximum is  $0.22 \times 2\pi$ , which is close to the theoretical value of  $0.21 \times 2\pi$ , and clearly below the  $0.5 \times 2\pi$  observed in conventional two-beam interferometers. Similar spectra can be recorded for a five-beam interferometer when using the  $6S_{1/2}, (F=4) \rightarrow 6P_{1/2}, (F'=4)$  transition, where the equivalent dark state consists of five magnetic sublevels. One observes five-beam interference signals [12] corresponding to the interference of five magnetic sublevels. Let us note that when orienting the optical beams in a counterpropagating geometry rather than a copropagating one, an atom interferometer with five spatially separated paths can be realized using three optical pulses. Multiple-beam atom interferometers have more recently been realized in other laboratories using other techniques [16–18].

Besides the fringe sharpening effect, further interesting effects occur in multiple-beam interference experiments when the phase difference between adjacent paths is not a constant for all paths. Such nonlinear phase terms lead, for example, to the Talbot images long known in near field optics [19, 20], where quadratic phase terms occur in the Fresnel approximation of the wave equation. In a multiple-beam interferometer, nonlinear phase terms cause collapse and revival effects of the fringe pattern. If adjacent paths are out of phase by  $2(n+1) \times \pi$  ( $n = 1, 2, \dots$ ), the fringe signal collapses. However, the signal is revived if the accumulated quadratic phase equals  $2n \times \pi$ . These non-linear phase terms can be due to the photon recoil in an atom interferometer [15, 17, 18] or an additionally applied potential [21].

In addition to in the experiments described in the next section, the technique of multiple-beam Ramsey spectroscopy could be used to measure small magnetic fields, or, when applying a strong static electric field, in experimental tests for a permanent electric dipole moment (EDM) of an atom [21]. Besides the increased resolution compared to experiments determining the splitting between two adjacent Zeeman sublevels, this technique can also have benefits in terms of systematic effects. Since terms scaling linearly and nonlinearly in  $m_F$  can be measured simultaneously, one expects that the

quadratic Stark effect – a significant source of systematic uncertainties in most atomic EDM experiments – could be better characterized in this scheme.

## 4 Studies of quantum decoherence

### 4.1 Initial measurements: state preparation

Our studies of quantum decoherence were based on photon scattering off a path of the multiple-beam Ramsey scheme. An important experimental issue remained to ensure that the required resonant optical pulse performed on the  $F = 4, m_F = 4 \rightarrow F' = 5, m_F = 5$  cycling transition did not affect the interference signal in an unwanted way. Most importantly, this pulse might a priori optically pump additional population into the state  $F = 4, m_F = 4$ , which would then give an additional background to the interference signal. The double microwave transfer, described in Sect. 2, allowed us to largely suppress excitation of the other paths, which were left in the lower ( $F = 3$ ) hyperfine state. As described earlier, a coherent superposition of different magnetic quantum numbers in this lower ground state is generated by the first optical Ramsey pulse, which is tuned to the  $F = 3 \rightarrow F' = 3$  transition of the cesium D1 line. When not applying any repumping laser, we expect to find a significant population also in the upper ( $F = 4$ ) hyperfine state after this pulse, arising from its initial population and atoms being hyperfine pumped into this state by the Ramsey pulse. We have recorded a series of microwave spectra with applied magnetic bias field to measure the population of the different Zeeman levels in this upper hyperfine ground state. Figure 5a shows a spectrum recorded after applying only the first Ramsey pulse; one observes all of the 15 possible microwave transitions between the different Zeeman sublevels. Let us point out that the used microwave power was adjusted to obtain maximum transfer

efficiency for the  $F = 3, m_F = 3 \rightarrow F = 4, m_F = 4$  component which corresponds to the peak on the right associated with the highest microwave frequency. The microwave power for the other transitions is not necessarily optimized and could to some extent account for the different peak heights. For the spectrum shown in Fig. 5b,  $\sigma^-$ -polarized repumping light tuned to the  $F = 4 \rightarrow F' = 4$  was additionally applied during and slightly after the first optical Ramsey pulse. The repumping laser optically pumps most of the population left in the  $F = 4$  hyperfine state to the  $m_F = -4$  sublevel (yielding a peak at the lowest side of the microwave spectrum), which is a dark state for the repumping laser. For the spectra shown in Fig. 5c and d, we additionally applied the  $\sigma^+$ -polarized resonant photon scattering laser to test if this pulse transfers atoms into other Zeeman states. For small power levels, we do not measure any observable optical pumping between the Zeeman states, as shown in Fig. 5c for a laser power of 0.28 mW and a 12  $\mu$ s pulse length. The optical pumping between those levels is suppressed by the comparatively small Clebsch–Gordan coefficients of transitions starting from negative Zeeman levels for  $\sigma^+$ -polarized light, as, for example, the  $F = 4, m_F = -4 \rightarrow F' = 5, m_F = -3$  component is a factor of 45 weaker than the cycling transition  $F = 4, m_F = 4 \rightarrow F' = 5, m_F = 5$ . Nevertheless, optical pumping certainly occurs for higher laser powers. Figure 5d gives a spectrum recorded at a laser power of 1.66 mW, where a small, but clearly visible peak corresponding to the  $m_F = 4$  state is observed. In the experimental runs where we implemented a coupling to the environment by this pulse, we kept the optical power well below 1.66 mW to avoid significant optical pumping.

### 4.2 Scattering photons off an interfering path

In the next experimental step, we moved on to scattering photons off an interfering path of the multiple-beam Ramsey experiment, and we applied the complete sequence of

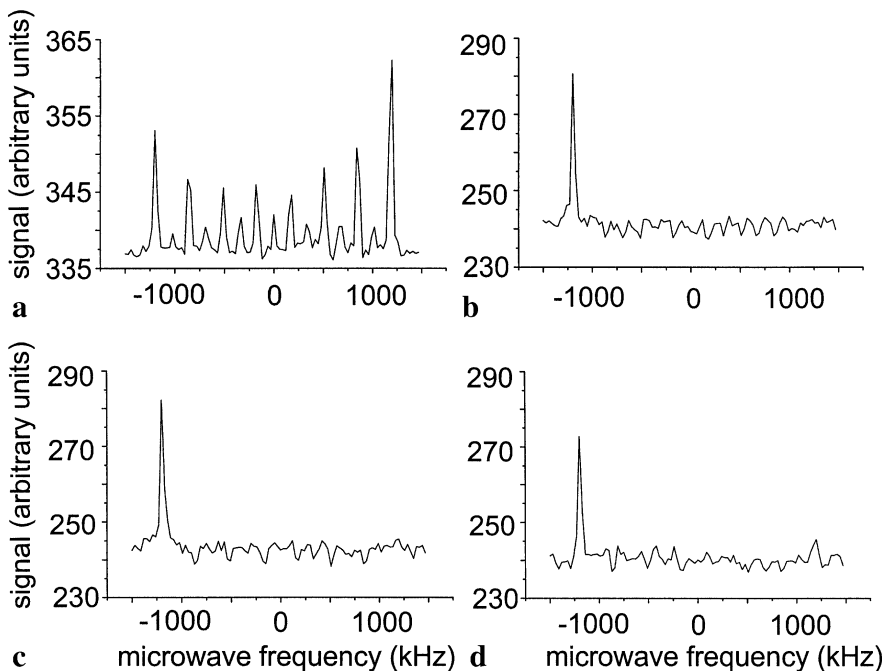


**Fig. 5a–d.** Microwave spectra in a magnetic bias field for different powers of the photon scattering laser. The plot gives the measured fluorescence signal from atoms transferred to the lower hyperfine ground state as a function of the applied microwave frequency, and allows the population in the different Zeeman sublevels of the upper ( $F = 4$ ) hyperfine ground state to be extracted. For the actual microwave frequency, one has to add an offset frequency of 9.192632 GHz. The spectra were recorded with: **a** no repumping light and no photon scattering beam; **b** with repumping light; **c** with repumping light and 0.28 mW power in the photon scattering beam; and **d** with 1.66 mW power in the photon scattering beam

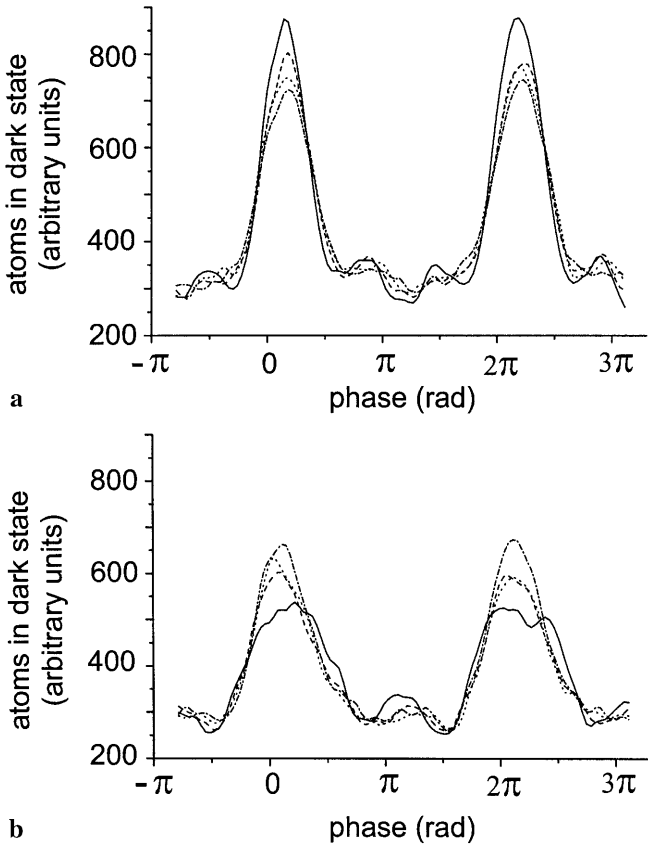


**Fig. 6a,b.** Multiple-beam interference fringes as a function of the phase of the second Ramsey pulse. The signals are shown for the different lengths of the optical pulse scattering photons from the  $m_F = 3$  path: without optical coupling pulse (*solid*), with an applied  $4 \mu\text{s}$  long optical pulse (*dashed*), with a  $6 \mu\text{s}$  long pulse (*dotted*) and with a  $9 \mu\text{s}$  long optical pulse (*dash-dotted*). **a** Signal measured with constant phase difference between adjacent paths. The fringe pattern loses contrast for longer pulse times. **b** In addition, a phase shift of  $\pi$  is applied to the  $m_F = 3$  path. Again, the spectra are shown for the same set of interaction times. Here, the contrast increases with larger interaction time. The principal maxima in **a** and **b** are slightly shifted from phases  $0$  and  $2\pi$ , because the difference of the two frequencies of the Ramsey pulses did not precisely match the energy splitting between the Zeeman substates

microwave and optical pulses described in Sect. 2. Figure 6 shows typical recorded multiple-beam interference patterns. For the spectra shown in Fig. 6a, the phase shift of the  $m_F = 3$  path due to the double microwave transfer has been compensated, and the phase difference between adjacent paths is constant for all paths. The solid line gives a fringe pattern measured without any attempt to keep track of an interfering path (i.e. no applied optical pulse resonant with the  $F = 4 \rightarrow F' = 5$  transition). One observes a sharply peaked four-way interference signal with two side peaks between the principal maxima. The background arises from the additional  $\sigma^-$ -polarized repumping light tuned to the  $F = 4 \rightarrow F' = 4$  component of the cesium D2 line applied during and slightly after the first Ramsey pulse. When applying an optical pulse to scatter photons from the  $m_F = 3$  path, we measure fringe signals as shown by the dashed line ( $4 \mu\text{s}$  long pulse), by the dotted line ( $6 \mu\text{s}$  long pulse) and by the dash-dotted line ( $9 \mu\text{s}$  long pulse). With increasing length of the optical pulse, the measured signal loses contrast. This is similar to what is observed in conventional two-beam

atom interferometers. However, the contrast for this four-beam interference signal does not approach zero for large photon scattering, as the three remaining beams can still interfere phase-coherently. One experimentally observes that the widths of the principal maxima increase and the signal becomes more and more similar to that of a three-path interference pattern. The spectra shown in Fig. 6b were recorded without compensating for the phase shift from the double microwave transfer, such that the  $m_F = 3$  path is phase shifted by  $\pi$  respectively to the other paths, as in the theoretical plot of Fig. 2b. With no photon scattering (*solid* line), the observed fringe contrast is significantly smaller than that observed for the spectrum of Fig. 6a. When scattering photons off the  $m_F = 3$  path, the counterintuitive situation occurs that the interference contrast increases. Again, the dashed line corresponds to a  $4 \mu\text{s}$  long optical pulse, the dotted to a  $6 \mu\text{s}$  long pulse and the dash-dotted line to a  $9 \mu\text{s}$  long pulse. Qualitatively speaking, the destructive interference of the  $m_F = 3$  path with the other paths is replaced by a more and more incoherent contribution of the path to the fringe pattern. When the photon scattering laser is fully applied, one expects the same interference patterns with and without an additional phase shift of the  $m_F = 3$  path. The experimental signals show this correspondence qualitatively for the longest pulses.

An analysis of the experimental signals shows that the measured fringe patterns are slightly broader than the theoretical ones (shown in Fig. 2), which we believe to be mainly due to magnetic fields inhomogeneities. Furthermore, the finite transfer efficiency of the microwave  $\pi$  pulses of roughly 70% causes deviations mainly for the signal with negative  $a$ , where the two microwave pulses are applied with the same phase. At present, the  $\pi$ -pulse efficiency is believed to be limited by a spatially inhomogeneous microwave field. Imperfections in the microwave pulse area partly cancel when the second pulse is applied with a  $\pi$  phase shift (as done for the spectra with positive values of  $a$ ), since the second transfer pulse then has an effective pulse area of  $-\pi$ . Using a simple theoretical model, one finds that the finite transfer efficiency can – to the first order – be accounted for by assuming effective values for the parameter  $a$ , with  $|a| \leq 1$ . In the present experimental stage, the range of the effective parameter  $a$  that can be investigated is roughly between  $-0.4$  and  $1$ .

In order to quantify our results, we have recorded fringe patterns for various optical pulse lengths and examined the fringe contrast of the spectra. Let us point out that the definition of the contrast is not unique for multiple-beam interference signals. Contrast definitions based on the autocorrelation function have been introduced [22], and these also allow a quantitative description of signals with inverted contrast. Such an inverted contrast shows up in the theoretical signal with one path phase shifted by  $\pi$  in the absence of a “which-way” detection ( $a = -1$  in Fig. 2b). However, all our experimental spectra recorded so far have a principal maximum at zero phase and do not show a contrast inversion (mainly due to the finite efficiency of our microwave transfer pulses). We have analyzed our spectra using the most common definition of the contrast (or visibility) introduced by Michelson, which is

$$c_M = \frac{I_{\max} - I_{\min}}{I_{\max} + I_{\min}}, \quad (11)$$



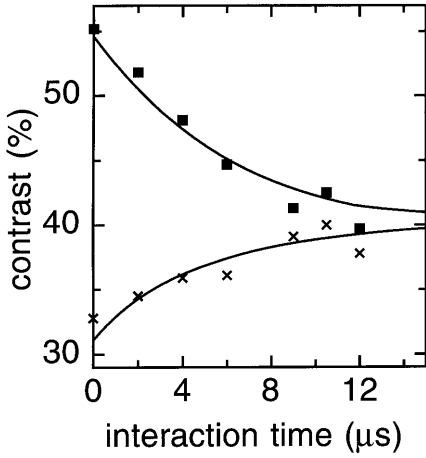


**Fig. 7.** Fringe contrast  $c_M$  of interference patterns recorded for different pulse lengths of an optical beam scattering photons off the  $m_F = 3$  path. The data points were measured without (squares) and with (crosses) a  $\pi$  phase shift of the  $m_F = 3$  path

where  $I_{\max}$  ( $I_{\min}$ ) denotes the maximum (minimum) value of the interference signal. The squares in Fig. 7 show the contrast of interference patterns recorded with constant phase differences between paths for different coupling to the environment of the  $m_F = 3$  path. This data was fitted with a theoretical model for the fringe contrast that is based on (8), and in addition accounts for a finite  $\pi$  pulse efficiency, an additional background caused by the repumping light, and a technical broadening of the interference fringes modeled by a Gaussian. As was already qualitatively seen in Fig. 6, the contrast decreases with a larger number of scattered photons off the  $m_F = 3$  path (solid curve) when there is a constant phase difference between all paths. A feature that is not present in conventional two-beam interferometers is shown by the crosses in Fig. 7, corresponding to data recorded with the  $m_F = 3$  path phase shifted by  $\pi$ . Here, the fringe contrast increases with photon scattering off the  $m_F = 3$  path. For a larger coupling to the environment, the contrast for the two different preparations converges to the same value, as was already shown qualitatively in Fig. 6.

#### 4.3 Decoherence and “path” information

The preceding section showed that the scattering of photons on a path of a multiple-beam interference experiment can – if the phase difference between adjacent paths is not constant for all paths – not only lead to a decrease but also to an increase of the fringe contrast. Obviously, in all cases (i.e. for the data recorded both with and without an additional phase shift of the  $m_F = 3$  path), there is a loss of coherence when scattering photons off a path. This suggests that in a multiple-beam interferometer the Michelson fringe contrast alone is not sufficient to quantify decoherence.

In order to obtain a further measure, we have attempted to estimate the “which-path” information that is contained in the emitted photons. This approach is inspired from discussions on complementarity in two-beam interferometers [1, 23, 24]. It is clear from information theory that the information that is lost in the atomic degrees of freedom when scattering photons off a path equals the “which-path” information obtainable

from the emitted photons. This in turn allows us to estimate the “which-path” information carried away by the photon field from the atomic signal. Mathematically, the escape of the photons can be described by performing a trace operation over the photon degrees of freedom, which has yielded the density matrix of (8).

To quantify the “which-path” information contained in the scattered photons, we follow earlier works [6, 10, 11] and introduce the path guessing likelihood  $L$ . This quantity gives the probability of determining the path of the atom in an interferometer when detecting the scattered photons with unity quantum efficiency. In a symmetric two-path interferometer, it is easy to see that the likelihood equals  $\frac{1}{2}$  and 1 for no “which-way” information and all possible “which-way” information respectively. However, the expected fringe contrast here equals unity for no possible “which-path” information and zero in the latter case. To account for the intermediate case of partial “which-path” detection in a two-beam interferometer, a relation between fringe contrast and path distinguishability has been developed [10]. For our four-beam interference arrangement, the optimum path guessing likelihood with no “which-path” detection equals the highest probability of finding an atom in a distinct Zeeman sublevel, corresponding to the maximum path weight  $(c_n^2)_{\max}$ . Using  $c_n^2 = \frac{5}{16}$  for states  $m_F = -3$  and 3 and  $c_n^2 = \frac{3}{16}$  for states  $m_F = -1$  and 1, we obtain  $(c_n^2)_{\max} = \frac{5}{16}$ . Certainly, one can improve the guessing likelihood when irradiating, for example, the  $m_F = 3$  path with light and detecting the scattered photons. A reasonable path guessing strategy then would be: when detecting a photon, choose  $m_F = 3$ , and if not, choose  $m_F = -3$ . This strategy yields a path guessing likelihood

$$L = \frac{5}{16} \cdot (1 + P_{\text{photon},3}), \quad (12)$$

where  $P_{\text{photon},3}$  denotes the probability for an atom in the path with  $m_F = 3$  to scatter a photon. From (7) it follows that  $P_{\text{photon},3} = 1 - a^2$ , which then links the expected fringe pattern (10) to the maximum possible value of the path guessing likelihood.

In order to derive the possible path guessing likelihood from our measured fringe patterns, we first estimate the modulus of the value of  $a$  from the spectra. As discussed earlier (Fig. 6), the fringe signals with and without an applied  $\pi$  phase shift for the path in  $m_F = 3$  differ considerably for no scattering of photons ( $|a| = 1$ ), whereas for large photon scattering (i.e.  $|a| \ll 1$ ) the fringe signal hardly changes when introducing this phase shift. In the latter case the  $m_F = 3$  path only contributes incoherently to the fringe pattern, while it contributes coherently when  $|a|$  is close to unity. Let us define the presumed modulus of  $a$  at a given pulse time of the photon scattering laser as

$$a_p = \frac{I_+(\varphi = 0) - I_-(\varphi = 0)}{(I_+(\varphi = 0) - I_-(\varphi = 0))_{\max}}, \quad (13)$$

where  $I_+$  and  $I_-$  denote the measured fringe signals with and without an applied  $\pi$  phase shift of the  $m_F = 3$  path. Further,  $(I_+ - I_-)_{\max}$  specifies the maximum difference of the signals, i.e. the differential signal measured without photon scattering. When we additionally account for a constant background to the fringe pattern  $K = (N/2)[(1/c_{M,\max}) - 1]$ , as estimated

from the Michelson fringe contrast  $c_{M,\max}$  measured with no scattering of photons and a constant phase between paths, we find

$$L_{a_p} = \frac{1}{1+K} \left( c_3^2 + \frac{K}{N} \right) \left[ 1 + (1 - a_p^2) \right] \quad (14)$$

as an estimate for the maximum possible guessing probability using the above described strategy. This enables us to quantify the “which-path” information that is carried away by the photon field solely from a measurement of the atomic degrees of freedom. Note that this approach relies on our model for the fringe pattern, as we at present do not apply full quantum tomography of the atomic quantum state.

It should be stressed that the maximum value of  $L$  depends on the basis that has been chosen for the betting strategy, as has been pointed out in [10, 14]. In our case, the strategy described so far corresponds to a “which-path” measurement in the detection basis of the photon vacuum state  $|D_2\rangle$  and an orthogonal state  $|D_{20}\rangle$  with one or more photons. However, the basis in which  $L$  reaches its maximum value is in general given by a coherent superposition of the eigenstates of the detection basis. One can show that in this optimum basis the guessing probability  $L_{a_p}$  is given by (14) with the term  $1 - a_p^2$  replaced by  $\sqrt{1 - a_p^2}$ . From that value, the path distinguishability can be derived. However, it is not immediately clear how a measurement in this rotated basis could be performed experimentally when one of the basis states corresponds to a continuum state. This optimum case can certainly be realized when the “which-path” information is decoded, for example, in an additional internal atomic state [6].

The presumed value for the path guessing likelihood  $L_{a_p}$ , as extracted from our data, is shown in Fig. 8 for different photon scattering pulse times. The solid circles give values derived for the detection basis. As expected, the likelihood, being a measure for the possible “which-path” information contained in the photons, increases for larger pulse length. Extracting the value of  $a$  from our data gives the presumed value. If we instead base our analysis on a use of the optimum basis and replace the term  $1 - a_p^2$  in (14) by  $\sqrt{1 - a_p^2}$ , we obtain the open circles in Fig. 8. Both data sets in Fig. 8 have been fitted with a theoretical model that is based on (14).

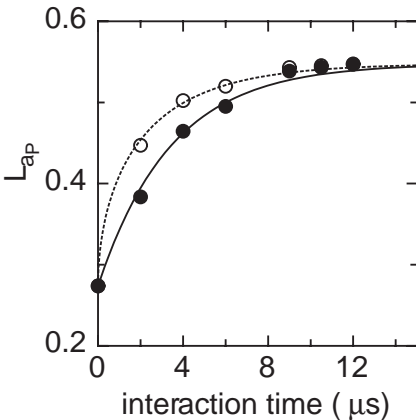


**Fig. 8.** Presumed path guessing likelihood in the detection basis (solid circles) and the theoretically optimum basis (open circles)

Finally, we wish to point out that our experiment can be seen as a model system for the study of controlled decoherence in quantum systems, as, for example, quantum logic gates. In quantum computation science, the study of decoherence is of high interest, as such experiments aim towards the realization of complex entangled quantum systems (see, for example, [25]). For such “larger size” quantum systems, an understanding of the role of decoherence becomes increasingly important. In our experiment, the four paths of the Ramsey interference setup can represent two-quantum bits, and, from a quantum information science viewpoint, the  $\pi$  phase shift of the  $m_F = 3$  path performed for some of the measurements equals the operation of a phase gate, which is an elementary quantum gate. It is appropriate to argue that the photon scattering corresponds to the coupling to an engineered reservoir (see also [9]). For large couplings, this results in an output state that is independent of the input parameters of the quantum gate.

## 5 Conclusion

We performed a study of quantum decoherence in a multiple-beam generalization of a Ramsey interference experiment. The experiment was performed by scattering photons off one of the four interfering paths. In contrast to the situation observed for two-beam interferometers, the scattering of photons on a path can here not only lead to a decrease but also sometimes to an increase of the Michelson fringe contrast, depending on the circumstances. This suggests that in the multiple-beam case the Michelson contrast is not sufficient to quantify decoherence. The results are in agreement with a density matrix calculation. In all cases, the atomic quantum state loses information with light scattering, as the emitted photons carry away “which-path” information. A measure of this information is a key issue in such considerations. We used the presumed path guessing likelihood to quantify the amount of “which-path” information contained in the emitted photons, which involves the measurement of more than a single output state of the interferometer. For the future, an important issue would be to detect the photons scattered by the atoms with high quantum efficiency, as this would permit a direct verification of the derived path guessing likelihood. A further perspective would be to extend the measurements towards an interferometer with an increased number of interfering paths, or also other quantum systems of larger size.

*Acknowledgements.* We wish to thank T.W. Hänsch, H. Walther, and B.-G. Englert for helpful discussions. This work was supported in parts by the Deutsche Forschungsgemeinschaft and within the frame of a European Community science program.

## References

1. J.A. Wheeler, W.H. Zurek (Eds.): *Quantum Theory and Measurement* (Princeton University Press, New Jersey 1983)
2. R. Feynman, R. Leighton, R. Sands: *The Feynman Lectures on Physics*, Vol. III (Addison Wesley, Reading 1965)
3. T. Pfau, S. Spälter, C. Kurtsiefer, C.R. Ekstrom, J. Mlynek: *Phys. Rev. Lett.* **73**, 1223 (1994)
4. J.F. Clauser, S. Li: *Phys. Rev. A* **50**, 2430 (1994)



5. M.S. Chapman, T.D. Hammond, A. Lenef, J. Schmiedmayer, R.A. Rubenstein, E. Smith, D.E. Pritchard: *Phys. Rev. Lett.* **75**, 3783 (1995)
6. S. Dürr, T. Nonn, G. Rempe: *Phys. Rev. Lett.* **81**, 5705 (1998)
7. W.H. Zurek: *Phys. Today* **44**, 36 (1991)
8. M. Arndt, O. Nairz, J. Vos-Andreae, C. Keller, G. van der Zouw, A. Zeilinger: *Nature (London)* **401**, 680 (1999)
9. C.J. Myatt, B.E. King, Q.A. Turchette, C.A. Sackett, D. Kielpinski, W.M. Itano, C. Monroe, D.J. Wineland: *Nature (London)* **403**, 269 (2000)
10. B.-G. Englert: *Phys. Rev. Lett.* **77**, 2154 (1996)
11. W.K. Wootters, W.H. Zurek: *Phys. Rev. D* **19**, 473 (1979)
12. M. Weitz, T. Heupel, T.W. Hänsch: *Phys. Rev. Lett.* **77**, 2356 (1996)
13. M. Mei, M. Weitz: *Phys. Rev. Lett.* (in press)
14. B.-G. Englert: private communication
15. M. Weitz, T. Heupel, T.W. Hänsch: *Europhys. Lett.* **37**, 517 (1997)
16. H. Hinderthür, A. Pautz, F. Rieger, F. Ruschewitz, J.L. Peng, K. Sengstock, W. Ertmer: *Phys. Rev. A* **56**, 2085 (1997)
17. S.B. Cahn, A. Kumarakrishnan, U. Shim, T. Sleator, P.R. Berman, B. Dubetsky: *Phys. Rev. Lett.* **79**, 784 (1997)
18. L. Deng, E.W. Hagley, J. Denschlag, J.E. Simsarian, M. Edwards, C.W. Clark, K. Helmerson, S.L. Rolston, W.D. Phillips: *Phys. Rev. Lett.* **83**, 5407 (1999)
19. K. Patorski: *Progress in Optics XXVII*, ed. by E. Wolf (North-Holland, Amsterdam 1989) p. 1
20. J.F. Clauser, S. Li: *Phys. Rev. A* **49**, R2213 (1994); M.S. Chapman, C.R. Ekstrom, T.D. Hammond, J. Schmiedmayer, B.E. Tannian, S. Wehinger, D.E. Pritchard: *Phys. Rev. A* **51**, R14 (1995)
21. M. Mei, T.W. Hänsch, M. Weitz: *Phys. Rev. A* **61**, 020101(R) (2000)
22. E.G. Steward: *Fourier Optics* (Ellis Horwood, Chichester 1989)
23. N. Bohr: *Albert Einstein: Philosopher-Scientist*, ed. by P.A. Schilpp (Library of Living Philosophers, Evanston 1949) p. 200
24. T. Hellmuth, H. Walther, A. Zajonc, W. Schleich: *Phys. Rev. A* **35**, 2532 (1987); and references therein
25. A.M. Steane: *Rep. Prog. Phys.* **61**, 117 (1998)